Received: 16 January 2022 | Revised: 28 February 2022 | Accepted: 16 March 2022

DOI: 10.1111/jwas.12885

ORIGINAL RESEARCH

Journal of the World Aquaculture Society Open Access | WORLD AQUACULTURE Society | WILEY

Development of new real-time PCR methods for detection of *Decapod iridescent virus 1* in shrimp

Melony J. Sellars | **Louise Franz** | **Ralf Joachim Moser**

Genics Pty Ltd, St Lucia, Queensland, Australia

Correspondence
Melony J. Sellars, Genics Pty Ltd., Level 5, Gehrman Building, 60 Research Road, St Lucia, QLD 4067, Australia.
Email: melony.sellars@genics.com.au

Abstract

Novel Decapod Iridescent virus (DIV1) infections emerged in mainland China around 2014 and have devastated shrimp aquaculture operations in Chinese coastal provinces. In 2020, DIV1 has spread to Taiwan with devastating results to shrimp and crayfish farms, in addition to being found in wild caught *Penaeus monodon* from the Indian Ocean. This trend is a major cause for concern and an urgent reminder to expand the tools needed to monitor the spread of DIV1 globally. Here, we describe a set of four different real-time polymerase chain reaction (PCR) assays positioned across the genome of DIV1 to detect the virus in shrimp tissues. All four assays show a wide dynamic range and high analytical sensitivity and specificity. In addition, the newly developed assays show excellent diagnostic sensitivity and specificity in clinical *Litopenaeus vannamei* samples of North Asian origin. The new molecular toolset will enhance global capabilities to monitor the spread of DIV1 and ultimately be used as an early warning system for farmers and authorities to engage in appropriate risk mitigation strategies.

KEYWORDS
Decapod iridescent virus 1, Iridovirus, real-time PCR, Shrimp MultiPath Xtra

1 | INTRODUCTION

Since it was first mentioned in 1993 by two independent groups (Lightner & Redman, 1993; Montanie, Bonami, & Comps, 1993), suspected Iridovirus infections in members of the order Decapoda were only reported by Tang et al. (2007) within a timeframe of 20 years. Yet, the identification, isolation, and genomic characterization of two new pathogenic iridoviruses in redclaw crayfish *Cherax quadricarinatus* (*Cherax quadricarinatus* iridovirus [CQIV]) (Li, Xu, & Yang, 2017; Xu, Wang, Li, & Yang, 2016) and in *Litopenaeus vannamei* (Shrimp hemocyte iridescent virus [SHIV]) in December 2014 (Qiu et al., 2017; Qiu, Chen, Wang, et al., 2018) seemed to mark the re-emergence of a concerning outbreak trend of iridovirus infections in South-East Asia. Phylogenetic assessment of genomic and deduced protein sequence data led to the reclassification of the newly identified iridoviruses CQIV and SHIV to be part of the new genus *Decapodiridovirus* in the family Irodoviridae (Chinchar et al., 2018). In fact, both CQIV and SHIV were assessed to be different strains of the same viral species *Decapod iridescent* virus 1 (DIV1). Both DIV1 viruses contain a linear double-stranded DNA genome with a size of 165,695 bp (CQIV) and 165,809 bp (SHIV) (Li et al., 2017; Qiu, Chen, Wang, et al., 2018). DIV1 infects hematopoietic tissue, gills, and hepatopancreas of its host and leads to symptoms like empty stomach, a degree of discoloration on the surface of the hepatopancreas and softening of the shell leading to an overall high mortality of infected individuals (Qiu et al., 2017; Xu et al., 2016).

While deadly DIV1 outbreaks were mainly confined to coastal provinces of China (Kearns, 2020), it has since spread to shrimp and crayfish farms in Taiwan (The Fish Site, 2020). Interestingly, DIV1 has recently been detected in wild caught *Penaeus monodon* broodstock specimens in the Indian Ocean without any clinical signs of disease (Srisala et al., 2021). This in turn is lending to the concern that *P. monodon* might potentially be a host for DIV1 with the inherent risk to spread this emerging pathogen throughout the Asia-Pacific region.

Several PCR-based molecular methods targeting a limited number of viral hypothetical genes have been described (Table 1). Qiu et al. (2017) and Srisala et al. (2021) have opted to use nested PCR approaches targeting the viral ATPase gene and the major capsid protein (MCP) to detect the virus. Both currently available TaqMan real-time PCR approaches are targeting the viral ATPase gene (Gong et al., 2021; Qiu, Chen, Wan, et al., 2018). Two loop-mediated isothermal amplification methods (LAMPs) described by Chen et al. (2019) and Gong et al. (2021) are detecting the RNA polymerase II and ATPase, respectively, while a recently published recombinase polymerase amplification method focuses on MCP (Chen et al., 2020).

This study aims to expand the molecular tools portfolio for DIV1 detection with three novel SYBR real-time PCR assays directed at three new target genes spreading across the assembled genome from shrimp hemocyte iridescent virus isolate 20141215 (MF599468; Table 2). Based on the assembly, the putative target genes are ORF 51R (putative papainase gene), ORF 124R (putative cell surface gene), and ORF 114R (putative D5 family NTPase ATPase gene), which are also used in other studies referenced above. These new real-time PCR assays provide a broader gene target assay range for biosecurity agencies, regulators, and the global shrimp industry to better monitor and mitigate the risks posed by this emerging pathogen, DIV1.

2 | MATERIALS AND METHODS

2.1 | Sample collection and nucleic acid extraction

L. vannamei pleopod samples were collected from live individual shrimp taken from an earthen pond suffering mortalities in Northern Asia. Shrimp samples were submerged in 70% Laboratory Grade Ethanol for preservation and subsequent total nucleic acid (TNA = RNA and DNA) extraction. TNA was extracted using a MagMAX™ Core nucleic acid purification kit with the KingFisher FLEX robot (Thermo Fisher Scientific, CA) as described by Moser, Franz, Firestone, and Sellars (2022). Extracted sample TNA was eluted in 50 μl PCR grade water and directly used for the different analyses.

TABLE 1 Decapod Iridescent virus (DIV)-1 assays and corresponding primer sequences used in previous studies

Method	Target gene	Accession #	Host species	Name	Sequence 5′→3′	Amplicon size [bp]	LOD	References
Nested PCR	ATPase	KY681040.1	*Litopenaeus vannamei*	SHIV-F1/SHIV-R1	GGGCGGGAGATGGTGTTAGAT/ TCGTTTCGGTACGAAGATGTA	457	36 fg DNA	Qiu et al. (2017)
				SHIV-F2/SHIV-R2	CGGGAAACGATTCGTATTGGG/ TTGCTTGATCGGCATCCTTGA	129		
	Major capsid protein (MCP)	KY681039.1	*Penaeus monodon*	DIV1-F576/ DIV1-R576	TAGCAGCTTCGGAGCATTGA/ GCAAGGTTCCTCAGGTTGGA	576	NA	Srisala et al. (2021)
				DIV1-F409/ DIV1-R576	TAATCGGCAGTCATCACGGG/ GCAAGGTTCCTCAGGTTGGA	409		
TaqMan PCR	ATPase	KY681040.1	*L. vannamei*	SHIV-F/SHIV-R	AGGAGAGGGAAATAACGGGAAAAC/ CGTCAGCATTTGGTTCATCCATG	188	4 copies/ reaction	Qiu et al. (2018)
				TaqMan probe	FAM-CTGCCCATCTAACACC ATCTCCCGCCC-TAMRA			
	ATPase	KY681040.1	*L. vannamei*	DIV1-F/DIV1-R	AGGAAAGGAAACGAAAGAAATTATACC/ GCTTGATCGGCATCCTTGA	87	19 copies/μl	Gong et al. (2021)
				DIV1-P[a]	CACATGATTTGCAACAAGCTTCCAGCA			
LAMP	RNA Polymerase II (Pol II)	MF599468	*Exopalaemon carinicauda*	SHIV-FIP (F1C+F2)	TGGGGTTTCATATGGGCAAATGA TTTAAGAATGGAAAGATCCTATCAGC	217	NA	Chen et al. (2019)
				SHIV-BIP (B1C+B2)	AGGAGAAAAGGTTGGA TTGGTTACTTTTACT TCTGTTACTGCGATGG			
				SHIV-LF/ SHIV-LB	GAGAGGCGTGCAACTTTCTG/ TTTGGCATTGTCTGCT ACAATTTCC			
				SHIV-F3/SHIV-B3	GATGGCCATTCCTTCAAAC/ AAAATAGTCATCCTGAAATCCTT			
qLAMP	ATPase	KY681040.1	*L. vannamei*	FIP	CTCTTGATGGATACACTGATCT TCGGAGCCAGAGATTGTAACGG	364	190 copies/μl	Gong et al. (2021)
				BIP	ATTCAGTATTCAAGGA TTGGTTCAAAAGTTCTT CCATCTACCTCTC			

(Continues)

TABLE 1 (Continued)

Method	Target gene	Accession #	Host species	Name	Sequence 5′→3′	Amplicon size [bp]	LOD	References
				LF/LB	TTCGGTACGAAGATGTAGC/ GAAGAGTATCCTAAT ATGACCATCC			
				F3/B3	GGCTTGGTATCTTATTCAGAGAT/ ATTCACAACATCGTCACCAT			
RPA	MCP	KY681039.1	*L. vannamei*	RPA-F5/RPA-R5	CAGATCAGAGCGCATTCG ATCCCATAGGCACCGC/ CGTAAGAGAACATGTGGTAT CCGGTGAGTTCGGG	159	11 copies/ reaction	Chen et al. (2020)
				RPA-probe	ATACGAATCTTCAGATCGTATTCCCGTGA (FAM-dT)G(THF)C(BHQ1-dT) GCCGATTACTTCTC[P]			

Abbreviations: LAMP, loop-mediated isothermal amplification; LOD, limit of detection (unit varies); RPA, recombinase polymerase amplification.
[a]Fluorophore and quencher not specified.

TABLE 2 SYBR green real-time polymerase chain reaction (PCR) assays, primer sequences, and associated limit of detection (LOD) values described in this study

Target gene	Assay	Primer name	Primer sequences 5′→3′	Annealing temp [°C]	Amplicon size [bp]	LOD[a] [copies/reaction (Ct)	Sequence accession #	Note
ORF 51R–putative papainase gene	SYBR qPCR	DIV_PAP_01F	TCGCGAATTTCTCAACCGGA	60	104	2.5 (31.6)	MF599468.1 NC_055165	This study
		DIV_PAP_01R	TCTCAATGGACCACTTCCGC					
ORF 105R–putative patatin-like gene phospholipase	SYBR qPCR	DIV_PAT_01F	TGACAGACGATCAACGCGAA	60	105	1.7 (32.4)		
		DIV_PAT_01R	ACGGTTCGAAGATTAACGGGA					
ORF 114R–putative D5 family NTPase ATPase gene	SYBR qPCR	DIV_ATPase_01F	CAAACATGGGAGCTGCAAG	60	84	6.2 (32.7)		
		DIV_ATPase_01R	CGTCAGCATTTGGTTCATCC					
ORF 124R–putative cell surface gene	SYBR qPCR	DIV_CSG_01F	TATGCCAGGAGAGGCATGGA	60	110	1.9 (32.7)		
		DIV_CSG_01R	GCCTTTGACGTTCTCTTGACG					

[a]Limit of detection—copies per reaction (cycle threshold Ct value).

2.2 | PCR-based assay design and run parameters

A total of 10 real-time PCR assays targeting various open reading frames (ORF) from SHIV isolate 20141215 (Accession # MF599468) were selected for prescreening based on the following criteria:

- Putative function (ranging from potential pathogenicity to exotic functions)
- Distribution across the genome map of SHIV isolate 20,141,215 (Accession MF599468)
- BLAST analysis for each potential target ORF

All PCR assays developed in this study were designed using the PRIMER 3 software (Untergasser et al., 2012) as implemented in the NCBI interface (https://www.ncbi.nlm.nih.gov/tools/primer-blast/index.cgi?LINK_LOC=BlastHome). The final selection of four SYBR green based real-time PCR assays presented here target ATPase gene (DIV ATPase), patatin (DIV PAT), papainase (DIV PAP), and cell surface G (DIV CSG) and were chosen based on amplification efficiency, titration curve fit, linear dynamic range and melt curve analysis. These assays were further developed as diagnostic assays for monitoring DIV1 infections. Assays and corresponding primer sequences used in this study are listed in Table 2.

Real-time PCR assays were setup in 384-well PCR plates using the PowerUp SYBR Green Master Mix and run on the QuantStudio 12K Flex Real-Time PCR system (Thermo Fisher Scientific, CA) described elsewhere (Moser et al., 2022).

2.3 | Direct amplicon sequencing and sequence analysis

Real-time PCR amplicons were sequenced directly to confirm sequence authenticity. PCR amplicons in original amplification reaction mix/volume and corresponding forward and reverse primers (3.2 μM) were submitted to the Australian Genome Research Facility (AGRF, Brisbane Australia) for direct Sanger sequencing using Big Dye Terminator chemistry 3.1 and ABI Capillary Sequencer 3730xl (Thermo Fisher Scientific, CA).

The quality of sequence traces were checked and curated using the Sequencher Software (GeneCodes, MI) and verified sequences confirmed using the BLAST tool interface of NCBI (https://www.ncbi.nlm.nih.gov/home/about/; National Centre for Biotechnology Information, MD).

2.4 | Assay verification and validation

Real-time PCR assays and the commercially run Shrimp MultiPath™ service (Genics Pty Ltd, Brisbane Australia) were assessed against a list of performance criteria such as serial dilution and amplification efficiency assessment (qPCR), analytical parameters, and diagnostic parameters in line with the validation pathway recommended by the OIE (OIE, 2021).

2.4.1 | qPCR standard curve and amplification efficiency

Synthetic double-stranded DNA templates (GBlocks; Integrated DNA Technologies, IA) for each real-time PCR assay were sourced from Integrated DNA Technologies and diluted in a 10-fold dilution series spanning 10,000 copies per reaction down to 1 copy per reaction. Four replicates per dilution step were run and amplification efficiencies calculated using Equation (1).

$$Efficiency = 10^{\frac{-1}{slope}} - 1 \quad (1)$$

Slope is the log-linear phase of the standard titration curve.

2.4.2 | Analytical sensitivity and specificity

ASe, or the limit of detection (LOD), was determined via a dilution to extinction experiment and subsequent probit regression analysis. Synthetic templates for each corresponding qPCR assay were diluted in nonsymmetrical steps to reach extinction of the template in the lowest dilution steps. The following dilution steps were assessed (in copies per reaction): 100/50/25/12.5/10/6.25/5/2.5/1/0.5/0.1/0.05/0.005.

LOD was calculated via a probit regression analysis using MedCalc® Statistical Software version 20.019 (MedCalc Software Ltd, Ostend Belgium) and Equation (2) below.

$$probit(p) = a + b \times X \quad (2)$$

probit (p) = inverse standard normal cumulative distribution function Φ^{-1}

X = dose variable

a = regression coefficient Constant

b = slope of regression equation.

ASp was continuously assessed on synthetic template in clinical sample matrix background. Clinical samples used in this study additionally had a background of different pathogens, including Pir A toxin gene & Pir B toxin gene (AHPND/EMS; acute hepatopancreatic necrosis disease/Early mortality syndrome) and *Enterocytozoon hepatopenaei* (EHP) as confirmed by Shrimp MultiPath™ (Genics Pty Ltd, Brisbane, Australia). In addition, DIV1 qPCR assays were run against selected *L. vannamei* and *P. monodon* samples from two geographically diverse locations (Kenya and Vietnam; data not shown) with in-house confirmed hepatopancreatic parvovirus (HPV), infectious hypodermal and hematopoietic necrosis virus (IHHNV), monodon baculovirus (MBV), and Laem Singh virus (LSNV). Assays were also tested for cross-reactivity on polychaete worms from the genus *Perinereis* sourced from South-East Queensland, Australia.

2.4.3 | Diagnostic specificity and sensitivity

To estimate diagnostic parameters diagnostic specificity (DSp) and diagnostic sensitivity (DSe) for all four assays, a generic golden reference standard method was employed via the interface MICE (http://mice.tropmedres.ac/home.aspx) on a *L. vannamei* shrimp population of 91 specimens. The upper Ct range of each assay was chosen as LOD and cut-off for binary conversion of qPCR values. Each assay was chosen to serve as assumed gold reference standard and DSe and DSp calculated for subsequent comparison.

3 | RESULTS

The initial step of the assay verification and validation pathway was to measure the performance of each assay in a standard curve titration analysis. Key metrics are curve fit (R-square values) showing quality of technical replicates and amplification dynamic as well as slope of the regression line to calculate PCR efficiencies. All four novel assays for the detection of DIV1 (DIV-CSG, -PAT, -PAP, and -ATPase) show a tight curve fit with R-Square values greater

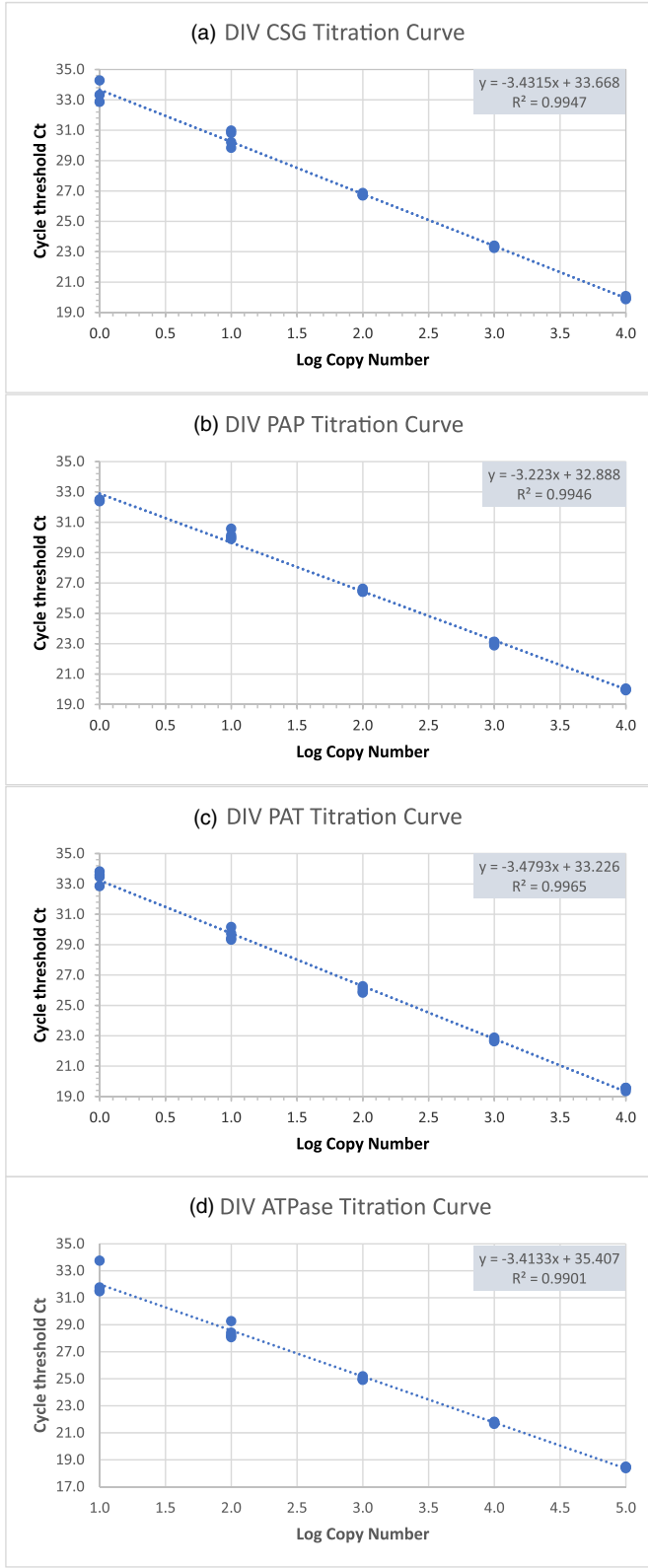

FIGURE 1 Legend on next page.

TABLE 3 Amplification efficiencies of qPCR assays

Assay	Slope	Efficiency[a]	Amplification efficiency [%]
DIV_PAP	−3.223	2.043	104.3
DIV_PAT	−3.479	1.938	93.8
DIV_ATPase	−3.413	1.963	96.3
DIV_CSG	−3.432	1.956	95.6

[a]Efficiency of 2 indicates perfect amplification dynamics with every cycle.

TABLE 4 Top BLAST hits for quantitative polymerase chain reaction (qPCR) amplicon sequences (direct amplicon sequencing forward and reverse) for qPCR assays Decapod Iridescent virus papainase (DIV PAP), Decapod Iridescent virus patatin (DIV PAT), Decapod Iridescent virus cell surface G (DIV CSG), and DIV ATPase

Assay	Top hit description	Query length [bp]	Max score	Total score	Query cover	E value	Per. Ident	Acc. Len	Accession
DIV PAP	Shrimp hemocyte iridescent virus isolate 20141215	103	187	187	100%	3.00E-44	100	165809	NC_055165.1
DIV PAT	Shrimp hemocyte iridescent virus isolate 20141215	102	185	185	100%	9.00E-44	100	165809	NC_055165.1
DIV CSG	Shrimp hemocyte iridescent virus isolate 20141215	107	194	194	100%	2.00E-46	100	165809	NC_055165.1
DIV ATPase	Shrimp hemocyte iridescent virus ATPase gene	83	150	150	100%	1.00E-33	100	1200	KY681040.1

Note: Shrimp hemocyte iridescent virus (SHIV) = Decapod iridescent virus 1 (DIV1).

TABLE 5 Probit regression analysis and limit of detection results for SYBR green quantitative polymerase chain reaction (qPCR) assays Decapod Iridescent virus (DIV) cell surface G (CSG), papainase (PAP), patatin (PAT), and ATPase

	Regression coefficients and *SEs*				Limit of detection LOD		
ASSAY	Concentration (b)	*SE* (b)	Constant (a)	Std. Error (a)	Copy per reaction (Ct value) $p = .95$	95% CI (Ct value)	
DIV CSG	0.987	0.187	−1.187	0.206	2.9 (32.1)	1.9 (32.7)	7.0 (30.8)
DIV PAP	1.055	0.200	−1.672	0.284	3.1 (31.3)	2.5 (31.6)	4.5 (30.8)
DIV PAT	1.308	0.250	−1.288	0.217	2.2 (32.0)	1.7 (32.4)	3.4 (31.4)
DIV ATPase	0.312	0.048	−1.026	0.183	8.6 (32.2)	6.2 (32.7)	15.7 (31.3)

0.99 along a dynamic range of 1 to 10,000 copies per reaction (Figure 1). The amplification efficiency for each of the assays is, DIV PAP 104.3%, DIV ATPase 96.3%, DIV CSG 95.6%, and DIV PAT 93.8% (Table 3). All four assays were

FIGURE 1 Standard curve assessment via serial dilution of Decapod Iridescent virus cell surface G (DIV CSG) (a), Decapod Iridescent virus papainase (DIV PAP) (b), Decapod Iridescent virus patatin (DIV PAT) (c), and DIV ATPase (d) showing tight curve fit (R2 value) and regression equation

TABLE 6 Binary input data presented as frequency profile counts (each assay as positive or negative) for diagnostic sensitivity (DSe) and specificity (DSp) estimation using a standard golden reference approach with all assays subsequently used as reference

qPCR assays				
ATPase	**CSG**	**PAP**	**PAT**	**Frequency observed**
Positive	Positive	Positive	Positive	30
Positive	Positive	Positive	Negative	0
Positive	Positive	Negative	Positive	2
Positive	Positive	Negative	Negative	0
Positive	Negative	Positive	Positive	1
Positive	Negative	Positive	Negative	0
Positive	Negative	Negative	Positive	0
Positive	Negative	Negative	Negative	0
Negative	Positive	Positive	Positive	2
Negative	Positive	Positive	Negative	1
Negative	Positive	Negative	Positive	1
Negative	Positive	Negative	Negative	0
Negative	Negative	Positive	Positive	1
Negative	Negative	Positive	Negative	0
Negative	Negative	Negative	Positive	0
Negative	Negative	Negative	Negative	53
			Total	91

Note: The table is a list of all possible positive/negative combinations and tallies the count for each combination observed. For example, combination of all assays calling a sample POSITIVE is thirty.

further validated with respect to their analytical performance. For analytical specificity (ASp) samples positive for DIV1 were confirmed positive (100% inclusivity) and direct amplicon sequencing and database interrogation employed to validate the confirmed results (Table 4). Moreover, *L. vannamei* and *P. monodon* samples negative for DIV1 but positive for other shrimp pathogens such as HPV, IHHNV, MBV, LSNV, *Vibrio parahaemolyticus* (PirA/PirB) and EHP showed no false positive DIV1 assay results (exclusivity). No cross-reactivity of all new qPCR assays has also been confirmed with polychaete worm samples from the genus *Perinereis* (data not shown).

Analytical sensitivity or LOD was determined to be 2.2 copies/reaction (Ct = 32.0; DIV PAT), 2.9 copies/reaction (Ct = 32.1; DIV CSG), 3.1 copies/reaction (Ct = 31.3; DIV PAP), and 8.6 copies/reaction (Ct = 32.2; DIV ATPase) (Table 5).

Diagnostic metrics sensitivity (DSe) and DSp were based on the traditional golden reference assay approach with each assay evaluated as golden reference point to determine the differential DSe and DSp values for each of the novel DIV1 assays using a single population of 91 *L. vannamei* shrimp samples known to be infected with DIV1. The binary qPCR profile for all samples (Table 6) was established and formed the basis for the DSe/DSp assessment. With DIV ATPase set as golden reference assay 100% DSe/100% DSp, the results for the other assay were obtained as 97%/93.1% (DIV CSG), 93.9%/93.1% (DIV PAP), and 100%/93.1% (DIV PAT), respectively. Setting DIV CSG as reference 100% DSe/100% DSp, all comparative assays were 88.9%/98.2% (DIV ATPase), 91.7%/96.4% (DIV PAP), and 97.2%/96.4% (DIV PAT). DIV PAP as reference yielded DSe/DSp results 88.6%/96.4% for DIV ATPase, 94.3%/94.6% for DIV CSG, and 97.1%/94.6% for DIV PAT. Finally, DIV PAT as golden reference assay resulted in a DSe/DSp of 89.2%/100% for DIV ATPase, 94.6%/98.1%, for DIV CSG, and 91.9%/98.1% for DIV PAT.

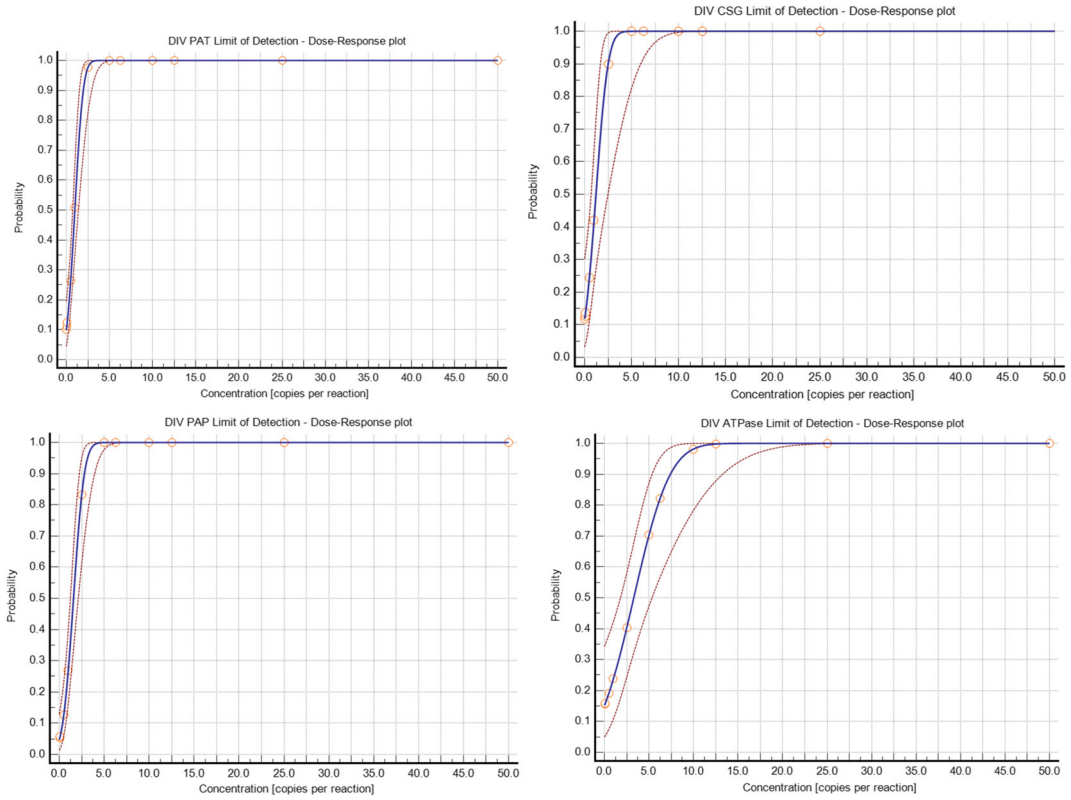

FIGURE 2 Probit regression analysis curve fit with 95% confidence interval (dotted line) shown to determine the limit of detection (LOD) for Decapod Iridescent virus patatin (DIV PAT), papainase (PAP), cell surface G (CSG), and ATPase. Sixteen replicates were tested at each concentration point and dose (cut-off copy number per reaction) determined at probability of 0.95

4 | DISCUSSION

The sudden occurrence of mass mortality among farmed Penaeid shrimp caused by DIV1 infections in China in 2014 (Li et al., 2017; Qiu et al., 2017; Xu et al., 2016) sparked an urgent need to detect and monitor the infectious agent DIV1 to protect the global shrimp farming industry from this emerging biosecurity risk. This included known and potential risks such as uncooked commodity shrimp and fresh frozen polychaetes used in shrimp maturation diets.

A handful of DIV1 target assays against a limited amount of target loci have been described (Table 1) leaving an acute need for more tools to detect and monitor the virus spread worldwide. Qiu et al. (2017) and Srisala et al. (2021) have opted to use nested PCR approaches targeting the viral ATPase gene and the MCP to detect the virus. Both currently available TaqMan real-time PCR approaches are targeting the viral ATPase gene (Gong et al., 2021; Qiu, Chen, Wan, et al., 2018). Two loop-mediated isothermal amplification methods (LAMP) described by Chen et al. (2019) and Gong et al. (2021) are detecting the RNA polymerase II and ATPase, respectively, while a recently published recombinase polymerase amplification method focuses on MCP (Chen et al., 2020).

The assays DIV PAT, DIV PAP, and DIV CSG, developed in this study are aimed at expanding the assay and target portfolio for DIV1 detection and monitoring (Table 2). A separate DIV ATPase qPCR assay was also developed in this study as a strong primer dimer peak was observed when running the TaqMan capture primers published by Qiu, Chen, Wan, et al. (2018) in SYBR and melt-curve analysis mode (data not shown).

TABLE 7 Diagnostic sensitivity and specificity estimates from a basic golden reference assay approach for SYBR green quantitative polymerase chain reaction (qPCR) assays Decapod Iridescent virus cell surface G (DIV CSG), papainase (PAP), patatin (PAT), and ATPase

Parameters	Test A assumed perfect gold standard (%)[a]	Test B was assumed as a perfect gold standard (%)[a]	Test C was assumed as a perfect gold standard (%)[a]	Test D was assumed as a perfect gold standard (%)[a]
Prevalence	36.3 (26.6–47.1)	39.6 (29.6–50.4)	38.5 (28.6–49.3)	40.7 (30.6–51.5)
DIV ATPase (Test A)				
Sensitivity	100	88.9 (73.0–96.4)	88.6 (72.3–96.3)	89.2 (73.6–96.5)
Specificity	100	98.2 (89.0–99.9)	96.4 (86.6–99.4)	100 (91.7–100)
PPV	100	97.0 (82.5–99.8)	93.9 (78.4–98.9)	100 (87.0–100)
NPV	100	93.1 (82.5–97.8)	93.1 (82.5–97.8)	93.1 (82.5–97.8)
DIV CSG (Test B)				
Sensitivity	97.0 (82.5–99.8)	100	94.3 (79.5–99.0)	94.6 (80.5–99.1)
Specificity	93.1 (82.5–97.8)	100	94.6 (84.2–98.6)	98.1 (88.8–99.9)
PPV	88.9 (73.0–96.4)	100	91.7 (76.4–97.8)	97.2 (83.8–99.9)
NPV	98.2 (89.0–99.9)	100	96.4 (86.4–99.4)	96.4 (86.4–99.4)
DIV PAP (Test C)				
Sensitivity	93.9 (78.4–98.9)	91.7 (76.4–97.8)	100	91.9 (77.0–97.9)
Specificity	93.1 (82.5–97.8)	96.4 (86.4–99.4)	100	98.1 (88.8–99.9)
PPV	88.6 (72.3–96.3)	94.3 (79.5–99.0)	100	97.1 (83.4–99.9)
NPV	96.4 (86.6–99.4)	94.6 (84.2–98.6)	100	94.6 (84.2–98.6)
DIV PAT (Test D)				
Sensitivity	100 (87.0–100)	97.2 (83.8–99.9)	97.1 (83.4–99.9)	100
Specificity	93.1 (82.5–97.8)	96.4 (86.4–99.4)	94.6 (84.2–98.6)	100
PPV	89.2 (73.6–96.5)	94.6 (80.5–99.1)	91.9 (77.0–97.9)	100
NPV	100 (91.7–100)	98.1 (88.8–99.9)	98.1 (88.8–99.9)	100

[a]Gold standard model assumed that test A is perfect (100% sensitivity and 100% specificity; all patients with gold standard test positive are diseased and all patients with gold standard test negative are nondiseased). Values shown are estimated means with 95% confidence interval.

All four SYBR qPCR assays showed tight titration curve characteristics across a wide dynamic range spanning 1–10,000 copies of template per reaction (range expanded to 10^6 copies per reaction—data not shown) with close to perfect amplification efficiencies ranging from 93.8 to 104.3% (Table 3; Figure 1). The LOD for DIV PAT at 2.2, DIV CSG at 2.9, DIV PAP at 3.1, and DIV ATPase at 8.6 copies per reaction (Tables 2 and 4, Figure 2) indicates that all assays are highly sensitive compared to reported TaqMan and LAMP assays available (Table 1). The LOD of the TaqMan assays was reported at slightly higher levels compared to the four new assays with 4 copies per reaction (Qiu, Chen, Wan, et al., 2018) and 19 copies per μl (Gong et al., 2021). In addition, the LOD for the LAMP assay (Gong et al., 2021) was reported at 190 copies per μl. The newly described RPA method (Chen et al., 2020) showed a sensitivity of 11 copies per reaction using a probit regression approach. No ASe data were presented for the nested PCR assays, and only a positive detection rate of the virus ranging from 15.2% in *Fenneropenaeus chinensis* (33 specimens) to 15.5% in *L. vannamei* (575 specimens) and 5 out of 10 specimens of *Macrobrachium rosenbergii* was reported (Qiu et al., 2017). The newly presented assays show a comfortable range of sensitivity compared to other published assays and could arguably be the method of choice when selecting a laboratory medium complexity-based approach that is cost-effective (SYBR real-time PCR) to monitor DIV1 (Tables 1 and 2).

In line with aforementioned studies, ASp has been assessed to be 100% in samples with a background of various shrimp pathogens, and no cross-reactivity has been detected for polychaete worm samples tested. Specificity has further been confirmed through direct amplicon sequencing of each qPCR amplicon for PAT, PAP, CSG, and ATPase and sequence authenticity annotated using the NCBI BLAST search tool confirming 100% sequence identity with the intended target (Table 5).

A population of 91 *L. vannamei* shrimp samples from Northern Asia-Pacific shrimp farms, suspected to be infected with DIV1, were analyzed for DIV1 infection status in this study, and the diagnostic performance of each assay was assessed using a golden standard reference approach (Tables 6 and 7). All assays show good diagnostic performance with high sensitivity and specificity. In the differential comparison, qPCR assay DIV PAT reaches on average highest diagnostic sensitivity while maintaining a high level of specificity. On the contrary, Assay DIV ATPase showed highest specificity but a lower sensitivity. Overall, the presented assay performance is comparable to Qiu, Chen, Wan et al. (2018) who reported a DSe and DSp of 95.3 and 99.2%, respectively, for their TaqMan qPCR test from 323 DNA samples analyzed.

5 | CONCLUSION

DIV1 is a critical emerging pathogen threat for the global shrimp industry, and all necessary steps need to be taken to avoid spread of the disease into the Asia-Pacific region and beyond. Hence, one key approach is to develop novel target gene and assays for this emerging pathogen and increase molecular tool capability for national and international biosecurity efforts. The novel targets and assays presented in this study are a vital step toward the tool expansion and will serve as a key foundation for increasing biosecurity preparedness. In particular, the DIV PAT and DIV PAP assays provide two new tools with high specificity and sensitivity toward monitoring and detecting this pathogen.

ACKNOWLEDGMENTS

The authors would like to thank the Board of Genics Pty Ltd Australia for investing in core R&D to allow development of these essential tools to mitigate disease risk and increase biosecurity awareness of our global shrimp industry.

CONFLICT OF INTEREST

The authors declare no conflicts of interest.

AUTHOR CONTRIBUTIONS

Melony J. Sellars concepted and wrote the manuscript and organized funding. **Louise Franz** executed laboratory experiments and proof-read the manuscript. **Ralf Joachim Moser** concepted scientific experiments, executed laboratory work, undertook statistical analysis, and wrote the manuscript.

ORCID

Ralf Joachim Moser https://orcid.org/0000-0003-2721-7616

REFERENCES

Chen, Z., Huang, J., Zhang, F., Zhou, Y., & Huang, H. (2020). Detection of shrimp hemozyte iridescent virus by recombinase polymerase amplification assay. *Molecular and Cellular Probes*, *49*, 1–8.

Chen, X., Qiu, L., Wang, H., Zou, P., Dong, X., Li, F., & Huang, J. (2019). Susceptibility of *Exopalaemon carinicauda* to the infection with shrimp hemocyte iridescent virus (SHIV 20141215), a strain of Decapod iridescent virus 1 (DIV1). *Viruses*, *11*, 387.

Chinchar, G.; Yang, F.; Huang, J.; Williams, T.; Whittington, R.; Jancovich, J., … Marschang, R. (2018) *One new genus with one new species in the subfamily Betairidovirinae*. International Committee on Taxonomy of Viruses (ICTV). Retrieved from https://talk.ictvonline.org/files/ictv_official_taxonomy_updates_since_the_8th_report/m/animal-dna-viruses-and-retroviruses/8051

Gong, H.-Y., Li, Q.-Y., Zhang, H., Ye, L., Shi, L., & Feng, Y.-H. (2021). Development and comparison of qPCR and qLAMP for rapid detection of the decapod iridescent virus 1 (DIV1). *Journal of Invertebrate Pathology*, *182*, 1–7.

Kearns, M. (2020). *Deadly shrimp virus has farmers in China fearing the worst*. SeafoodSource. https://www.seafoodsource.com/news/aquaculture/deadly-shrimp-virus-has-farmers-in-china-fearing-the-worst

Li, F., Xu, L., & Yang, F. (2017). Genomic characterization of a novel iridovirus from redclaw crayfish *Cherax quadricarinatus*: Evidence for a new genus within the family Iridoviridae. *The Journal of General Virology*, *98*, 2589–2595.

Lightner, D. V., & Redman, R. M. (1993). A putative iridovirus from the penaeid shrimp *Protrachypene precipua* Burkenroad (Crustacea: Decapoda). *Journal of Invertebrate Pathology*, *1*, 107–109.

Montanie, H., Bonami, J. R., & Comps, M. (1993). Irido-like virus infection in the crab *Macropipus depurator* L. (Crustacea, Decapoda). *Journal of Invertebrate Pathology*, *61*, 320–322.

Moser, R. J., Franz, L., Firestone, S. M., & Sellars, M. J. (2022). *Enterocytozoon hepatopenaei* real-time and shrimp MultiPath™ PCR assay validation for South-East Asian and Latin American strains of Penaeid shrimp. *Diseases of Aquatic Organisms*. (in press). https://doi.org/10.3354/dao03655

OIE – World Organisation for Animal Health. (2021). *Standard operating procedure for OIE registration of Diagnostic kits*. https://www.oie.int/app/uploads/2021/06/a-sop-may-2021.pdf

Qiu, L., Chen, M. M., Wan, X. Y., Li, C., Zhang, Q. L., Wang, R. Y., … Huang, J. (2017). Characterization of a new member of *Iridoviridae*, Shrimp hemocyte iridescent virus (SHIV), found in white leg shrimp (*Litopenaeus vannamei*). *Scientific Reports*, *7*, 11834.

Qiu, L., Chen, M. M., Wan, X. Y., Zhang, Q. L., Li, C., Dong, X., … Huang, J. (2018). Detection and quantification of shrimp hemozyte iridescent virus by TaqMan probe based real-time PCR. *Journal of Invertebrate Pathology*, *154*, 95–101.

Qiu, L., Chen, M. M., Wang, R. Y., Wan, X. Y., Li, C., Zhang, Q. L., … Huang, J. (2018). Complete genome sequence of shrimp hemocyte iridescent virus (SHIV) isolated from white leg shrimp, *Litopenaeus vannamei*. *Archives of Virology*, *163*, 781–785.

Srisala, J., Sanguanrut, P., Thaiue, D., Laiphrom, S., Siriwattano, J., Khudet, J., … Sritunyalucksana, K. (2021). Infectious myonecrosis virus (IMNV) and Decapod iridescent virus 1 (DIV1) detected in captured, wild *Penaeus monodon*. *Aquaculture*, *545*, 737262.

Tang, K. F. J., Redman, R. M., Pantoja, C. R., Groumellec, M. L., Duraisamy, P., & Lightner, D. V. (2007). Identification of an iridovirus in *Acetes erythraeus* (Sergestidae) and the development of *in situ* hybridization and PCR method for its detection. *Journal of Invertebrate Pathology*, *96*, 255–260.

The Fish Site. (2020.). *Deadly decapod virus confirmed in Taiwan*. The Fish Site. Retrieved from https://thefishsite.com/

Untergasser, A., Cutcutache, I., Koressaar, T., Ye, J., Faircloth, B. C., Remm, M., & Rozen, S. G. (2012). Primer3-new capabilities and interfaces. *Nucleic Acids Research*, *40*, e115.

Xu, L. M., Wang, T., Li, F., & Yang, F. (2016). Isolation and preliminary characterization of a new pathogenic iridovirus from redclaw crayfish *Cherax quadricarinatus*. *Diseases of Aquatic Organisms*, *120*, 17–26.

How to cite this article: Sellars, M. J., Franz, L., & Moser, R. J. (2022). Development of new real-time PCR methods for detection of *Decapod iridescent virus 1* in shrimp. *Journal of the World Aquaculture Society*, 1–14. https://doi.org/10.1111/jwas.12885